

Effect of the carrier-envelope phase of the driving laser field on the high-order harmonic attosecond pulse

Zhinan Zeng, Ruxin Li, Wei Yu, and Zhizhan Xu

*Laboratory for High Intensity Optics, Shanghai Institute of Optics and Fine Mechanics, Chinese Academy of Sciences,
P. O. Box 800-211, Shanghai 201800, People's Republic of China*

(Received 17 June 2002; published 30 January 2003)

The effect of the carrier-envelope phase of a few-cycle driving laser field on the generation and measurement of high-order harmonic attosecond pulses is investigated theoretically. We find that the position of the generated attosecond soft-x-ray pulse in the cutoff region is locked to the oscillation of the driving laser field, but not to the envelope of the laser pulse. This property ensures the success of the width measurement of an attosecond soft-x-ray pulse based on the cross correlation between the attosecond pulse and its driving laser pulse [M. Hentschel *et al.*, *Nature (London)* **414**, 509 (2001)]. However, there still exists a timing jitter of the order of tens of attoseconds between the attosecond pulse and its driving laser field. We also propose a method to detect the carrier-envelope phase of the driving laser field by measuring the spatial distribution of the photoelectrons induced by the attosecond soft-x-ray pulse and its driving laser pulse.

DOI: 10.1103/PhysRevA.67.013815

PACS number(s): 42.65.Ky, 32.80.Rm

I. INTRODUCTION

In the physical picture of high-order harmonic generation (HHG) [1], a laser driven electron first escapes from the atomic core by tunneling through the Coulomb barrier. Once free, it oscillates freely in the laser field. When it is driven back to the core, it recombines with the core and emits a harmonic photon. With a many-cycle laser pulse, the maximum kinetic energy gained by the electron is $3.17U_p$, where U_p is the quiver energy of the free electron in the oscillating field. This defines the highest energy of the harmonic spectrum as $I_p + 3.17U_p$, where I_p is the ionization potential. But for harmonic generation using a few-cycle laser pulse, the situation can be different, e.g., no explicit cutoff and the appearance of harmonic intensity fluctuations [2], because the laser pulse is too short and the carrier-envelope phase [3] becomes a very important parameter.

The phase sensitivity of the high-order harmonics for very short driving laser pulses has been investigated theoretically in recent years [2,4]. For a few-cycle laser pulse, the carrier-envelope phase will greatly affect the HHG in the cutoff region. In Ref. [2], the authors considered whether the harmonics in the cutoff are resolved or not, and the different periodicity of the spectrum with a carrier-envelope phase of 0 and $\pi/2$. The intensity of the harmonics in the cutoff will also be affected by the carrier-envelope phase. In the investigation of the time profile of the harmonics, the authors of Ref. [2] found that there is a timing jitter among the attosecond pulses generated by laser pulses with different carrier-envelope phases. In Ref. [4], which investigated the phase sensitivity by considering the propagation effect, the authors also suggest that the timing jitter and the intensity fluctuations introduced by the phase sensitivity will present a severe limitation in attosecond measurements.

The generation of ultrashort pulses is a key to exploring the dynamic behavior of matter on ever shorter time scales. For example, several fundamental atomic processes, such as inner-shell electronic relaxation or ionization by optical tun-

neling, take place within a fraction of the oscillation period of visible or near-infrared radiation, which require very short probes for diagnostics. Many methods have been proposed for generating attosecond pulses. Farkas and Toth first proposed a method to generate attosecond pulses based on Fourier synthesis of laser induced multiple harmonics [5]. Raman processing has also been used to generate ultrashort pulses [6]. Belenov *et al.* analyzed the dynamics of an intense ultrashort pulse in a Raman-active medium. They found some additional nonlinear effects when the pulse duration is short in comparison with the time Ω^{-1} , where $\hbar\Omega = E_2 - E_1$ is the energy difference between the levels participating in the Raman scattering. Yoshikawa and Imasaka proposed an approach to generate short pulses at terawatt levels based on a two-color stimulated Raman effect using a simple optical system. Harris and Sokolov suggested a technique for producing subfemtosecond pulses based on using electromagnetically induced transparency. Nazarkin *et al.* observed a highly efficient transformation of laser radiation into higher-order Stokes and anti-Stokes components in impulsively vibrationally excited gaseous SF₆. They proposed a regime of Raman frequency conversion for generation of subfemtosecond pulses. Kaplan proposed an approach based on multifrequency cascaded stimulated Raman scattering to generate subfemtosecond pulses. A Raman-active material can support solitons consisting of the pump laser wave and many Stokes and anti-Stokes components whose coherent interference gives rise to trains of ultrashort pulses. Zhavoronkov and Korn generated pulses with durations below 4 fs using the method of ultrafast molecular phase modulation with previously impulsively excited Raman-active gases. Bartels *et al.* demonstrated experimentally that, using impulsively excited rotational wave packets in CO₂, the bandwidth of a probe pulse is increased by a factor of 9. Ivanov and Gorkum put forward a scheme to generate single subfemtosecond pulses by using a laser pulse with time-dependent ellipticity [7]. High-order harmonic emission is extremely sensitive to the polarization of the incident light. A

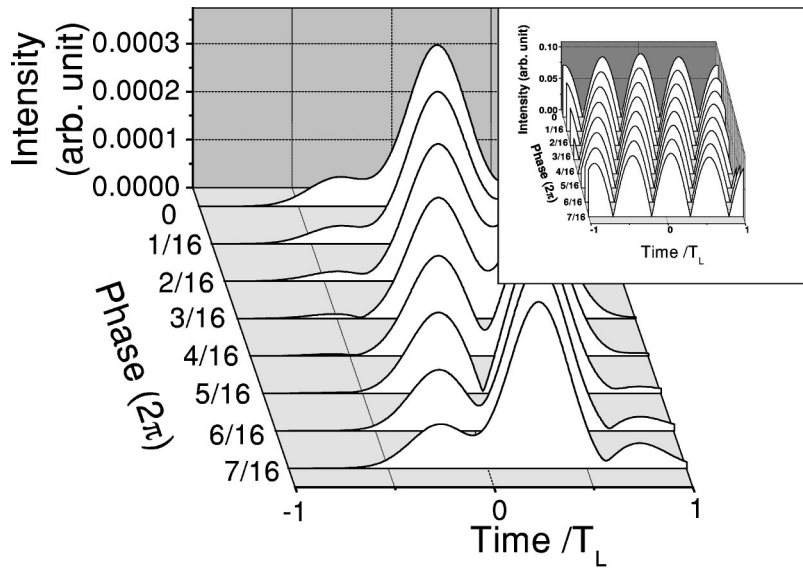


FIG. 1. The time profile of the attosecond pulses generated by a laser pulse of 7 fs, 800 nm, and $3.51 \times 10^{14} \text{ W/cm}^2$ with different carrier-envelope phases. The atom considered is helium. The photon energy of the soft-x-ray pulse is between 94 eV and 100 eV. Each attosecond pulse is produced by one half cycle near the peak of the envelope. Inset: $|E(t)|$ of the driving laser field. It shows that each half cycle is shifted along the temporal axis when the carrier-envelope phase is changed.

time-dependent ellipticity allows us to control the electron trajectories and produces emission only over a brief time interval. Antoine *et al.* also investigated the attosecond pulse trains produced by high-order harmonics theoretically [7]. They chose one of the trajectories of the electron by the propagation effect which leads to a train of pulses of extremely short duration. The method proposed by Christov *et al.* is more practical and convenient for generating attosecond pulses [8]. High-order harmonics were produced first by using few-cycle laser pulses and then a simple broadband x-ray filter was used to select some harmonics so the attosecond pulse could be obtained. Recently, there has been much progress on the experiment and theory of attosecond pulse generation and measurement [9,10].

Very recently a soft-x-ray pulse of the duration of 650 ± 150 as has been generated and measured [9]. With this attosecond pulse, the authors traced the electronic dynamics with a time resolution of ≤ 150 as. In the experiment, they also observed an attosecond synchronism of the soft-x-ray pulse with the carrier wave of the few-cycle driving laser. They speculated that the observed attosecond timing stability of the subfemtosecond x-ray pulse to its few-cycle driver is due either to a robustness of the high-harmonic generation process against variation of the carrier-envelope phase of the driving laser, or to a substantially reduced x-ray yield for values of the phase other than the optimum [9]. They believed that the latter cause is more reasonable and ascribed their experimental results to this possibility.

We have reinvestigated the effect of the carrier-envelope phase of the few-cycle driving laser field on the generation and measurement of high-order harmonic attosecond pulses. It was found that the position of the generated attosecond soft-x-ray pulse is locked to the oscillation of the driving laser field, but not to the envelope. This property ensures the success of the width measurement of an attosecond soft-x-ray pulse based on the cross-correlation method [9]. However, there still exists a timing jitter of the order of tens of attoseconds between the attosecond pulse and its driving laser field. We also propose a method to detect the carrier-envelope phase of the driving laser field by measuring the

spatial distribution of the photoelectrons induced by the attosecond soft-x-ray pulse and the driving laser field.

II. EFFECT OF THE CARRIER-ENVELOPE PHASE ON HHG

The approach of the investigation in this paper is similar to that in Ref. [2]. We calculated the dipole acceleration by numerically solving the time-dependent Schrödinger equation (TDSE). The laser pulse in the calculation is described by $E(t) = E_0(t) \cos(\omega_L t + \varphi_L)$, where ω_L is the frequency of the laser field, φ_L the carrier-envelope phase, and $E_0(t) = E_0 e^{-t^2/\tau^2}$ denotes the envelope of the laser pulse, where E_0 is the peak amplitude of the laser pulse and $\sqrt{2 \ln 2} \tau$ is its duration. The wavelength of the laser pulse is 800 nm. The dipole acceleration is then Fourier transformed to get the spectrum, and a time-frequency analysis (the Gabor analysis [11]) then reveals the time profile of the harmonics.

In Fig. 1, we show the time profiles of attosecond pulses for different carrier-envelope phases, obtained with a laser pulse whose duration is 7 fs and peak intensity is $3.51 \times 10^{14} \text{ W/cm}^2$. The atom considered is helium, whose ionization potential is 0.8996 a.u. (about 24.5 eV). The energy of the soft-x-ray pulse is between 94 eV and 100 eV, which is slightly above the cutoff defined by $I_p + 3.17 U_p$. We chose this energy for analysis because the shape of the attosecond pulse at this energy is relatively simple and can thus simplify our analysis without losing the physical point to be discussed in this work. First, we can see the same results as shown in Fig. 2 of Ref. [2], that there is a single pulse emission for $\varphi_L = 0$, whereas for $\varphi_L = \pi/2$ the harmonics is emitted twice. From these two cases, we can see the timing jitter and the harmonic intensity fluctuations as discussed in previous work [2,4].

Comparing Fig. 1 with its inset which shows $|E(t)|$ of the driving laser field, we can see the intrinsic reason that each soft-x-ray pulse comes from one half cycle of the laser oscillation. When the carrier-envelope phase of the laser pulse is changed, the time position of each half cycle is shifted. So

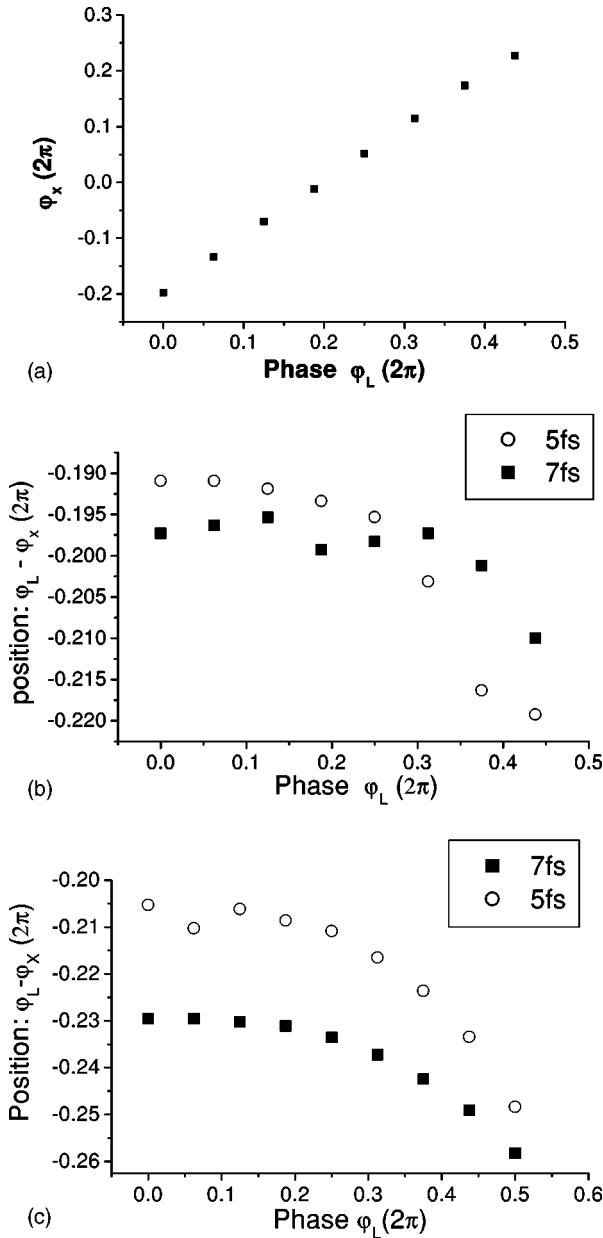


FIG. 2. The position of the attosecond pulse as a function of the carrier-envelope phase whose time profile is shown in Fig. 1. (a) The absolute position of the attosecond pulse as a function of the carrier-envelope phase. The shift is almost synchronous. Here, ϕ_x denotes the position of the attosecond pulse. If the attosecond pulse is generated at the envelope peak of the laser pulse, then $\phi_x = 0$. (b) The relative position of the attosecond pulse with respect to the laser oscillation as a function of a carrier-envelope phase, obtained by solving the TDSE. (c) The relative position of the attosecond pulse with respect to the laser oscillation as a function of the carrier-envelope phase, calculated with Corkum's model. Open circles and solid squares are for the 5 fs and the 7 fs driving laser pulses, respectively.

the position of the attosecond pulse is also shifted and locked to the laser oscillation. There is a very small timing jitter between the attosecond pulse and the laser oscillation. In Figs. 2(a) and 2(b), we show the absolute position of the attosecond soft-x-ray pulse and the relative position between

the attosecond pulse and the laser oscillation as a function of the carrier-envelope phase. From Fig. 2(b) we can see that the variation of the relative position with different carrier-envelope phase is very small, which means that the attosecond pulse is always generated at almost the same position of each half cycle of the laser pulse. The variation of the relative position (for 7 fs) is less than $0.018T_L$ (T_L is the laser period), or about 48 as. This result provides a good explanation for the experiment reported in Ref. [8]. Although the synchronism of the soft-x-ray pulse with the carrier wave of the few-cycle driving laser pulse permits a cross-correlation measurement, if we cannot control the carrier-envelope phase of the laser pulse, the randomness of the carrier-envelope phase will still limit the attosecond measurement when it is less than 100 as due to the timing jitter, which is as much as 48 as. For comparison, the timing jitter for the 5 fs driving pulse shown in Fig. 2(b) is about $0.03T_L$, which is larger than the timing jitter of the 7 fs laser pulse.

The origin of the timing jitter can be obtained by Corkum's model [1]. After tunneling, the electron motion is controlled by the equations

$$\frac{dv}{dt} = \frac{eE(t)}{m_e}, \quad (1a)$$

$$\frac{dx}{dt} = v. \quad (1b)$$

When $E(t)$ is a planar laser field (just a cosine function), the electron motion also has a period of T_L . But for a short laser pulse the trajectory of the electron motion is affected by the envelope of the laser pulse, e.g., in one half cycle, the electron with some kinetic energy has a trajectory l_1 and a free motion time t_1 ; then in the next half cycle, the electron with the same kinetic energy has a trajectory l_2 and a free motion time t_2 . Because of the envelope of the laser pulse $E_0(t)$, there is a difference between t_1 and t_2 , which is the origin of the timing jitter. For laser pulses with different carrier-envelope phases, the half-cycle oscillations have different time positions with respect to the peak of the envelope. Electrons with the same kinetic energy have different trajectories and free motion times, which results in the timing jitter of the attosecond pulses. A calculation based on Corkum's model indicates that the timing jitter [as shown in Fig. 2(c)] has a similar result to that from the TDSE [as shown in Fig. 2(b)], and the timing jitter is about $0.03T_L$ for the 7 fs pulse and $0.04T_L$ for the 5 fs pulse when the carrier-envelope phase changes from 0 to π . The shorter the duration of the laser pulse, the larger the timing jitter, because, when the duration of the laser pulse is shorter, the slope of the envelope $\partial E_0(t)/\partial t$ is larger and the difference of the free motion time of two adjacent half-cycle oscillations is larger. When the carrier-envelope phase is larger, $\phi_L - \phi_x$ in Fig. 2(b) and 2(c) is less and the timing jitter is larger. But when the carrier-envelope phase is large, the position of the attosecond pulse is far from the peak of the envelope and the intensity of the attosecond pulse becomes very small for a short laser pulse, which has no practical significance.

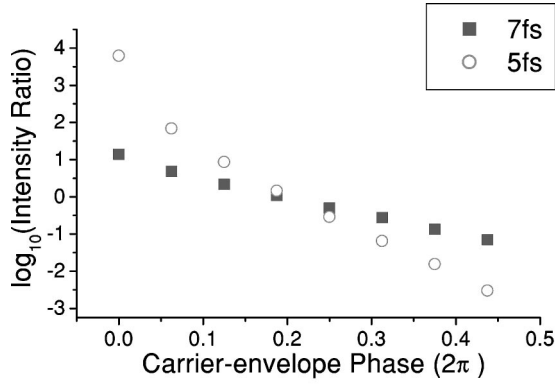


FIG. 3. The intensity ratio of two adjacent attosecond pulses around the envelope peak of the laser pulse. It shows that the intensity ratio is an exponential function of the carrier-envelope phase. Open circles and solid squares are for the 5 fs and the 7 fs driving laser pulses, respectively.

From Fig. 1 we can also see that the relative intensity of the two adjacent soft-x-ray pulses changes with the carrier-envelope phase. Figure 3 shows the intensity ratio of two adjacent soft-x-ray pulses generated around the envelope peak of the laser pulse. The logarithms of the intensity ratios are linear for different carrier-envelope phases, which means that the effect of the carrier-envelope phase on the intensity ratio is exponential. When $\varphi_L=0$, the intensity ratio of two adjacent attosecond pulses is very large (more than 10 for 7 fs pulse as shown in the figure). So it appears that there is only one pulse emission in the time profile. When $\varphi_L = \pi/2$, the intensity ratio of two adjacent attosecond pulses is near unity, and two pulses in the time profile appear.

The relation between the absolute intensity of the attosecond pulse and the carrier-envelope phase is very complex and it is very difficult to deduce an analytical result. But when the attosecond pulse is produced around the peak of the envelope, we can perform a simple analysis for the relative intensity of the two adjacent attosecond pulses. Our analysis is based on tunnel ionization, which is the first step of HHG, because in the following steps the motion of the electron is almost the same which will not affect the ratio greatly. (As mentioned above, the difference of the free motion time t_1 and t_2 is of the order of attoseconds, which is much less than the free motion time of $2/3T_L$. This means that the difference of two corresponding trajectories is very small.) The tunnel ionization of a hydrogenlike atom in a linearly polarized electric field is given by the Ammosov-Delone-Krainov theory [12] as follows:

$$w(E) = \frac{\omega_0}{2} C_{n^*l}^2 \frac{I_i}{2I_h} \frac{(2l+1)(l+|m|)!}{2^{|m|}(|m|)!(l-|m|)!} \times \left[2 \left(\frac{I_i}{I_h} \right)^{3/2} \frac{E_h}{|E|} \right]^{2n^*-|m|-1} \exp \left[-\frac{2}{3} \left(\frac{I_i}{I_h} \right)^{3/2} \frac{E_h}{|E|} \right]. \quad (2)$$

For two adjacent attosecond pulses produced around the peak of the envelope (in our calculation, this is defined as $t=0$),

$$I_1/I_2 \propto w(E_1)/w(E_2) \propto \exp \left[-\frac{2}{3} \left(\frac{I_i}{I_h} \right)^{3/2} \left(\frac{E_h}{|E_1|} - \frac{E_h}{|E_2|} \right) \right]. \quad (3)$$

Here I_i is the ionization potential of the atom and I_h is the ionization potential of hydrogen (about 13.6eV). E_1 and E_2 are the amplitudes of the laser electric fields. I_1 and I_2 are the intensities of two adjacent attosecond pulses. With Eq. (3) we can easily see that the intensity ratio is

$$I_1/I_2 \propto \exp \left[-\frac{2}{3} \left(\frac{I_i}{I_h} \right)^{3/2} \times E_h \frac{|E_0(t+T_L/2)\cos(\phi)| - |E_0(t)\cos(\phi)|}{|E_0(t+T_L/2)\cos(\phi)E_0(t)\cos(\phi)|} \right] \times \exp \left[-\frac{2}{3} \left(\frac{I_i}{I_h} \right)^{3/2} E_h \frac{1}{E_0(t+T_L/2)|\cos(\phi)|} \times (e^{t^2/\tau^2 - (t+T_L/2)^2/\tau^2} - 1) \right], \quad (4)$$

where t is the ionization time of the electron for the first attosecond pulse and ϕ is the phase of the electric field when the electron is ionized. When the carrier-envelope phase is changed, Eq. (4) can be written as

$$I_1/I_2 \propto \exp \left[-\frac{2}{3} \left(\frac{I_i}{I_h} \right)^{3/2} E_h \frac{1}{E_0[(\phi - \varphi_L)/\omega_L + T_L/2]|\cos(\phi)|} \times (e^{-[(\phi - \varphi_L)T_L/\omega_L + T_L^2/4]/\tau^2} - 1) \right] \times \exp \left[\frac{2}{3} \left(\frac{I_i}{I_h} \right)^{3/2} \frac{E_h}{E_0[(\phi - \varphi_L)/\omega_L + T_L/2]|\cos(\phi)|} \times [(\phi - \varphi_L)T_L/\omega_L + T_L^2/4]/\tau^2 \right]. \quad (5)$$

In Eq. (5) we use $e^x - 1 \approx x$ if $x \ll 1$, because around the peak of the envelope of the laser pulse t is very small compared to τ . So the change of the intensity ratio with the carrier-envelope phase can be expressed as an exponential function. From Eq. (5) we can also see that, when the duration of the laser pulse is shorter, the intensity ratio is larger (as shown in Fig. 3).

III. A SCHEME TO DETECT THE CARRIER-ENVELOPE PHASE

Since the relative intensity of two adjacent soft-x-ray pulses changes with the carrier-envelope phase, so if we produce free electrons using these two adjacent soft-x-ray pulses, the relative yield of the photoelectrons will be decided by the relative intensity of the attosecond pulses and

also by the carrier-envelope phase of the laser pulse. Based on this fact we propose a method to measure the carrier-envelope phase of the laser pulse. After the electron is set free by an x-ray photon, its motion is governed by the laser field. We can relate the final value $v_{\parallel,f}$ and the initial value $v_{\parallel,i}$ of the velocity component parallel to the laser polarization with the equation $v_{\parallel,f} = \sqrt{4U_p(t_d)/m} \sin(\omega_L t_d + \varphi_L) + v_{\parallel,i}$ [8]. (ω_L and φ_L are defined above. $U_p(t)$, t_d , and m are the ponderomotive energy, the time at which the electron is set free, and the electron mass, respectively, as in Ref. [8].) Because the time interval between two adjacent soft-x-ray pulses is $T_L/2$, the electrons produced by these two adjacent attosecond pulses acquire velocity components in opposite directions, e.g., if the final electron velocity for the first pulse is $\vec{V}_1 = \vec{V} + \vec{V}_{1i}$, the final electron velocity for the second one will be almost $\vec{V}_2 = -\vec{V} + \vec{V}_{1i}$, because the time interval is $T_L/2$ (corresponding to π) and $dE_0(t)/dt \ll E_0(t)\omega_L$, even for a 7 fs pulse [8]. Here \vec{V}_{1i} is the initial velocity of the photoelectron and \vec{V} denotes the velocity component acquired from the driving laser field. They have the same energy distribution after moving in the laser field, but different spatial distribution.

The scheme is shown in Fig. 4(a); it is similar to the scheme in Ref. [8] except that a microchannel plate (MCP) is used here to record the density distribution of the electrons instead of a kinetic energy spectrometer. First, the 7 fs pulse interacts with a gas jet to produce a train of pulses in the extreme ultraviolet and soft-x-ray spectral range. Then a filter is used to obtain the attosecond x-ray pulse, which will be used to ionize another gas, e.g., a Kr target. The electrons are set free at different instants by x-ray photons with different angle distributions in the presence of a laser field [8]. We found that these electrons will come out with different directions, although they have the same energy distribution.

In the calculation, we chose electrons with initial kinetic energy between 74 eV and 80 eV. (The initial kinetic energy of the free electron is decided by $W_0 = mv_i^2/2 = \hbar\omega_x - W_b$ [9], where W_b is the ionization potential energy of the atom. For simplicity, $W_b = 20$ eV is chosen in the calculation.) The laser pulse parameters are as given above. The electron is set free by an x-ray photon instantaneously in an arbitrary direction. The yield of photoelectrons is proportional to the intensity of the attosecond pulse. Then the MCP can detect the electrons with different directions, and Fig. 4(b) shows the peak position of the electron density distribution on the MCP while Fig. 4(c) shows the electron density distribution as a function of the carrier-envelope phase. The X axis denotes the position on the MCP in the polarization direction of the laser field. The position $X = 500$, the center of the slit, and the position where the electron is set free by the x-ray photon are collinear. When the carrier-envelope phase changes from 0 to 2π , Fig. 4(b) indicates that the peak position of the electron density distribution oscillates around the position $X = 500$ like a cosine function.

For a short laser pulse and its interaction with matter, the carrier-envelope phase is a very important parameter. In Ref. [3], Paulus *et al.* proposed a method to detect the carrier-envelope phase of a short pulse which is simpler than the

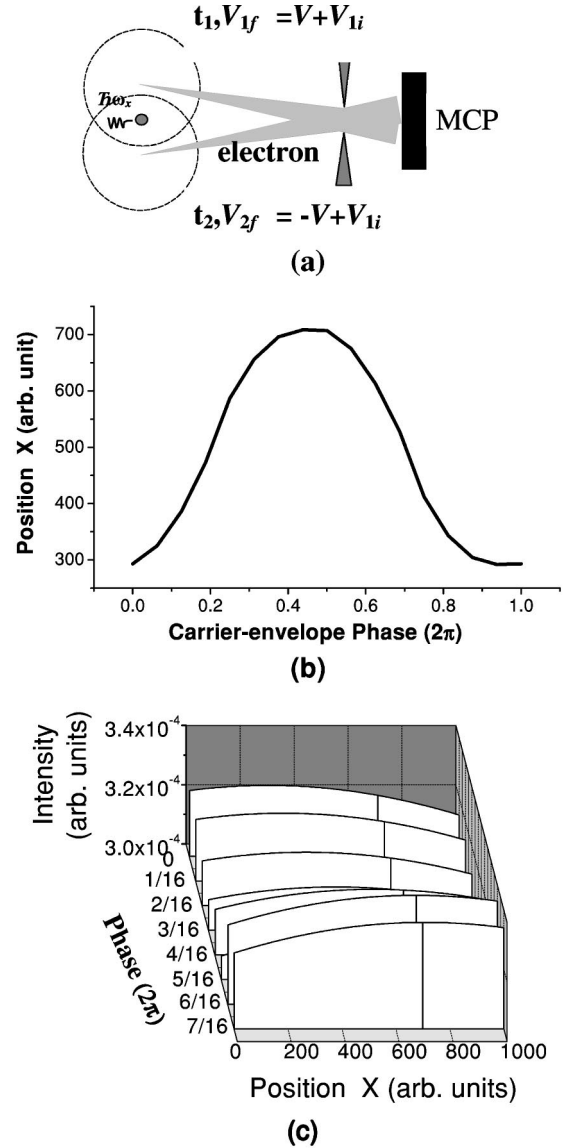


FIG. 4. (a) The schematic of the proposed scheme to measure the carrier-envelope phase. A microchannel plate (MCP) is used to detect the spatial distribution of the photoelectrons. The electron is ionized by the soft-x-ray pulse. After moving in the laser field, the electrons generated by two adjacent soft-x-ray pulses obtain velocity components in opposite directions from the laser field because the time interval of the two attosecond pulse is $T_L/2$. The electron density distribution can be recorded by the MCP and then the carrier-envelope phase can be inferred. (b) The peak position of the electron density distribution as a function of the carrier-envelope phase of the laser pulse. (c) One-dimensional simulation for the electron density distribution on the MCP.

scheme mentioned above. But for the generation, measurement, and application of an attosecond pulse, our scheme will be convenient for real-time detection of the carrier-envelope phase of the driving laser field.

We also investigated attosecond pulses with different photon energies in the cutoff region and different durations of the laser pulses (from 10 to 3 fs) and obtained similar results. We slightly changed the intensity of the laser field (by about

20) and also obtained similar results. In our calculation, the propagation effect was not taken into account.

IV. CONCLUSIONS

In conclusion, we performed a detailed analysis of the phase sensitivity of high-order harmonic generation using a few-cycle pulse. We found that the position of the attosecond soft-x-ray pulse is locked to the laser oscillation with a timing jitter of less than 48 as, which gives a good explanation for the experimental results reported in Ref. [9]. The ran-

domness of the carrier-envelope phase will still limit the attosecond measurement (although it is less than 100 as) if we cannot control the carrier-envelope phase accurately. We also found that the intensity ratio of two adjacent attosecond pulses changes with the carrier-envelope phase as an exponential function. Based on the change of the intensity ratio of two adjacent soft-x-ray pulses with the carrier-envelope phase, we proposed a method to measure the carrier-envelope phase of a driving laser field by measuring the spatial distribution of the photoelectrons induced by an attosecond soft-x-ray pulse and its driving laser pulse.

-
- [1] P. B. Corkum, Phys. Rev. Lett. **71**, 1994 (1993); P. Salieres *et al.*, *ibid.* **81**, 5544 (1998).
- [2] A. Bohan *et al.*, Phys. Rev. Lett. **81**, 1837 (1998).
- [3] T. Brabec and F. Krausz, Rev. Mod. Phys. **72**, 545 (2000); G. G. Paulus *et al.*, Nature (London) **414**, 182 (2001).
- [4] G. Tempea *et al.*, J. Opt. Soc. Am. B **16**, 669 (1999).
- [5] Gy. Farkas and Cs. Toth, Phys. Lett. A **168**, 447 (1992); S. E. Harris; *et al.*, Opt. Commun. **100**, 487 (1993).
- [6] E. M. Belenov *et al.*, JETP Lett. **55**, 218 (1992); S. Yoshikawa and T. Imasaka, Opt. Commun. **96**, 94 (1993); S. E. Harris and A. V. Sokolov, Phys. Rev. Lett. **81**, 2894 (1998); A. Nazarkin *et al.*, *ibid.* **83**, 2560 (1999); A. E. Kaplan, *ibid.* **73**, 1243 (1994); V. P. Kalosha and J. Herrmann, *ibid.* **85**, 1226 (2000); N. Zhavoronkov and G. Korn, *ibid.* **88**, 203901 (2002); R. A. Bartels *et al.*, *ibid.* **88**, 013903 (2002); A. V. Sokolov *et al.*, *ibid.* **87**, 033402 (2002);
- [7] M. Ivanov and P. B. Corkum, Phys. Rev. Lett. **74**, 2933 (1995); D. G. Lappas, and A. L'Huillier, Phys. Rev. A **58**, 4140 (1998); P. Antoine *et al.*, *ibid.* **56**, 4960 (1997); P. Antoine *et al.*, Phys. Rev. Lett. **77**, 1234 (1996); Nguyen Hong Shon *et al.*, Phys. Rev. A **63**, 063806 (2001).
- [8] I. P. Christov *et al.*, Phys. Rev. Lett. **78**, 1251 (1997); F. L. Kien *et al.*, Phys. Rev. A **58**, 3311 (1998).
- [9] M. Hentschel *et al.*, Nature (London) **414**, 509 (2001); M. Drescher *et al.*, Science **291**, 1923 (2001); P. M. Paul *et al.*, *ibid.* **292**, 1689 (2001).
- [10] M. Kitzler *et al.*, Phys. Rev. Lett. **88**, 173904 (2002); N. Milosevic *et al.*, *ibid.* **88**, 093905 (2002); J. Itatani *et al.*, *ibid.* **88**, 173903 (2002).
- [11] P. Antoine *et al.*, Phys. Rev. A **51**, R1750 (1995).
- [12] S. C. Rae and K. Burnett, Phys. Rev. A **46**, 2077 (1992).